Relating the 3D electrode morphology to Li-ion battery performance; a case for $LiFePO_4$

Liu, Zhao; Verhallen, Tomas W.; Singh, Deepak P.; Wang, Hongqian; Wagemaker, Marnix; Barnett, Scott

DOI
10.1016/j.jpowsour.2016.05.097

Publication date
2016

Document Version
Accepted author manuscript

Published in
Journal of Power Sources

Relating the 3D electrode morphology to Li-ion battery performance; a case for $LiFePO_4$

Zhao Liu[(1#)], Tomas W. Verhallen[(2#)], Deepak P. Singh[(2)], Sharon Wang[(1)], Marnix Wagemaker[(1)]* and Scott Barnett[(1)]

[(1)] Department of Materials Science and Engineering, Northwestern University, 2220 Campus Drive, IL 60208, Evanston, United States of America

[(2)]Department of Radiation Science and Technology, Delft University of Technology, Mekelweg 15, 2629JB, Delft, The Netherlands

* E-mail: m.wagemaker@tudelft.nl (tel: +31152783800, fax: +31152788303)
[#] Equally contributing authors

Abstract

One of the main goals in lithium ion battery electrode design is to increase the power density. This requires insight in the relation between the complex heterogeneous microstructure existing of active material, conductive additive and electrolyte providing the required electronic and Li-ion transport. FIB-SEM is used to determine the three phase 3D morphology, and Li-ion concentration profiles obtained with Neutron Depth Profiling (NDP) are compared for two cases, conventional $LiFePO_4$ electrodes and better performing carbonate templated $LiFePO_4$ electrodes. This provides detailed understanding of the impact of key parameters such as the tortuosity for electron and Li-ion transport though the electrodes. The created hierarchical pore network of the templated electrodes, containing micron sized pores, appears to be effective only at high rate charge where electrolyte depletion is hindering fast discharge. Surprisingly the carbonate templating method results in a better electronic conductive CB network, enhancing the activity of $LiFePO_4$ near the electrolyte-electrode interface as directly observed with NDP, which in a large part is responsible for the improved rate performance both during charge and discharge.

The results demonstrate that standard electrodes have a far from optimal charge transport network and that significantly improved electrode performance should be possible by engineering the microstructure.

Keywords: Li-ion batteries, charge transport, $LiFePO_4$, 3D imaging, FIB-SEM, Neutron Depth Profiling, electrode morphology.

1 Introduction

Driven by electrification of mobile transport key objectives in Li-ion battery research include improvement of the energy and power density, while ensuring a stable, long cycle life and the use of abundant and environmentally benign materials. A high energy density requires high lithium capacities of both positive and negative electrode materials and a large difference in potential. A larger power density, responsible for the (dis)charge time, requires a low internal resistance provided by facile charge transport, both ionic and electronic through the battery morphology.

The internal resistance of the battery is dominated by the resistance of the rate limiting charge transport step. This resistance causes the voltage polarization that scales with the (dis)charge current, leading to higher external potentials during charge and lower during discharge. This reduces the energy efficiency and moreover the effective capacity as the cell potentials are restricted by the stability window of the electrolyte to prevent detrimental electrolyte decomposition. Hence to reach higher currents and higher power densities, improvement of the rate limiting charge transport step is required. Alternatively, lowering the internal resistance allows to design thicker electrodes, increasing the relative amount of active materials in practical battery design, thereby increasing the effective energy density.

Li-ion battery electrodes based on liquid electrolytes typically consist of a solid state storage (active) material, an electron conducting phase, and a binder that together form the porous structure to be soaked with an organic electrolyte. As such, contributions to the internal resistance include (1) the electronic resistance of the contact between the active electrode material and current collector, (2) the

ionic network formed by the liquid electrolyte in the pores of the porous composite electrodes connecting the active electrode material and the electrolyte, (3) the charge transfer reaction between the liquid electrolyte and the active electrode material and (4) the solid state transport and phase nucleation/transformation kinetics within the active electrode material.{Ogihara, 2012 #682}

A large diversity of aspects have been reported to improve or be relevant for Li-ion battery (dis)charge kinetics each relating to one or more of these four contributions. This is well demonstrated for $LiFePO_4$, an important electrode material proposed by Padhi et al.{Padhi, 1997 #168} in 1997, and an intensively studied and well established model system. For $LiFePO_4$ the initial hurdle of poor intrinsic electronic and solid state ionic conduction were overcome by reducing the particle size in combination with carbon or metallic conductive coatings{Ravet, 1999 #222;Huang, 2001 #221;Herle, 2004 #378}.

Detailed investigation of the well-established first order phase transformation in $LiFePO_4$ has brought forward several interesting and relevant aspects for the charge transport. In particular in sub-micron crystallite sizes, the transformation has been suggested to proceed mainly via a particle-by-particle, or mosaic mechanism at low rates{Delmas, 2008 #274;Li, 2014 #656;Chueh, 2013 #542;Brunetti, 2011 #610} concentrating the current to a small fraction of the particles in an electrode, leading to large local differences in state of charge{Robert, 2013 #671;Ouvrard, 2013 #672}. For higher rates this moves gradually towards a more concurrent transformation of the particles at higher (dis)charge rates{Li, 2014 #656;Zhang, 2015 #742}. Recently it was shown that the end-member phases coexist even at low (dis)charge rates, transforming more concurrently than previously assumed{Zhang, 2015 #742} and that even in these sub-micron sized particles crack forming may limit the cycle life{Shapiro, 2014 #749;Yu, 2015 #746;Boesenberg, 2013 #750}. The predicted{Cogswell, 2012 #543;Malik, 2012 #434;Bai, 2011 #544} and observed solid solution{Zhang, 2014 #650;Zhang, 2015 #742;Liu, 2014 #665} and metastable phases{Orikasa, 2013 #599;Orikasa, 2013 #631}, induced by the overpotentials at high (dis)charge rates,

are considered to be responsible for the inherently fast (dis)charging of $LiFePO_4$ electrodes. The nucleation barrier for the first order phase transition in $LiFePO_4$ is predicted{Cogswell, 2013 #545} and observed{Zhang, 2015 #688;Robert, 2013 #671} to decrease for smaller particles and also the particle shape and nature of the surface has been recently shown to affect the transformation{Li, 2015 #744;Strobridge, 2015 #674}.

Direct observation of individual sub-micron $LiFePO_4$ particles show an increase in the transformation rate upon higher (dis)charge rates, for these rates qualitatively supporting a Butler-Volmer relation between charge transfer over the electrolyte-electrode interface and overpotential{Zhang, 2015 #742}, however the relatively slow transformation rates may also indicate that Butler-Volmer may not be followed at high overpotentials, supported by recent insights indicate that charge transfer over the electrolyte-electrode interface may be of crucial importance at higher overpotentials.{Bai, 2014 #691}

In many studies it has been recognized that, in sub-micron $LiFePO_4$, for higher rates the ionic transport through the porous electrode structure is rate limiting{Yu, 2006 #486;Jamnik, 2009 #334;Fongy, 2010 #421;Fongy, 2010 #422;Johns, 2009 #487;Zhou, 2006 #234;Gaberscek, 2006 #499;Gaberscek, 2007 #484;Robert, 2013 #751;Liu, 2010 #748;Strobridge, 2015 #747}. This is consistent with the direct observation that increasing the electrode loading density (proportional to the electrode thickness) results in a decrease in capacity at the same C-rate{Yu, 2006 #486;Singh, 2013 #555} and the observation that for thick electrodes particles near the electrolyte lithiate preferentially{Liu, 2010 #748;Robert, 2013 #751;Strobridge, 2015 #747}. However, studying the sequence of lithation of $LiFePO_4$ particles, Li et al.{Li, 2015 #673} show that the most resistive process in a $LiFePO_4$ electrode is the electronic conduction between the $LiFePO_4$ particle surface and the nearest branch of the percolating carbon network. Recently, direct observation of Li-ion concentration profiles as a function of the electrode depth indicated that the rate limiting process actually depends on the (dis)charge rate, for the

considered $LiFePO_4$ electrodes being nucleation at low rates, ionic transport through the electrolyte in the pores of the electrode at high rates, and most surprisingly electronic transport limitations at medium rates{Zhang, 2015 #688}.

From the forgoing it is evident that the overall charge transport properties of an electrode depends on the detailed 3D electrode morphology including: the porosity, tortuosity of both ionic and electronic conducting phases, active material grain size and shape. The diversity in reported results and the large amount of parameters involved make it difficult if not impossible to unambiguously establish the relation between the rate limiting step, the applied current and the electrode morphology, a prerequisite for reaching optimal kinetic battery performance. This has initiated several studies to reconstruct the 3D Li-ion battery electrode microstructure aiming to find a correlation with the electrode performance.

The benefits of characterizing 3D microstructure of Li-ion battery electrodes are two-fold. Firstly, it is considered an effective tool to quantitatively assess complex microstructural characteristics{Wilson, 2011 #32;Liu, 2013 #402;Chen-Wiegart, 2013 #403}. On the other hand, the 3D electrode reconstruction provides realistic microstructural input for 3D computational modeling of electrode electrochemical process{A. H. Wiedemann, 2013 #100;Hutzenlaub, 2014 #585}. Recently, 3D reconstruction resolving all three phases – oxide particles, carbonaceous materials, and electrolyte filled pores – has been achieved, allowing detailed quantitative analysis of the electrode transport property{Hutzenlaub, 2012 #612;Ender, 2011 #11;Ender, 2012 #589}. To date, although there are a few reports on three-phase 3D microstructure of $LiFePO_4$ electrode{Ender, 2012 #589;Ender, 2011 #11}, limited analysis was performed to investigate the correlation between electrode 3D microstructure with charge transport mechanisms. This analysis is hindered by the large number of variables that together determine the microstructure and the following transport properties. Ideally this number is reduced by

preparing electrodes of similar structure which fundamentally differ on a few key aspects, thereby isolating certain properties and their effect on the electrochemical properties.

In a recent study we have used a cheap and scalable templating technique, based on carbonate templates, improving the high rate capacity retention significantly in both $LiFePO_4$ and $Li_4Ti_5O_{12}$ electrodes{Singh, 2013 #555;Singh, 2013 #326}. Importantly, the applied templating method leads to only a marginal increase in the porosity, resulting in a combination of large tap density (high volumetric energy density) and improved power density. Interpretation of the electrochemical data has indicated an improved tortuosity of the electrolyte network throughout the electrode, a better ionic wiring provided by increased interconnectivity of the electrolyte filled pores in the electrode as induced by the template[22,31]. Surprisingly, also an improvement of the electronic conductivity was suggested, which could not be explained by the applied templating approach. The importance of the electronic conductivity in battery electrodes was also recently demonstrated by the direct observation of Li-concentration profiles, probed by operando Neutron Depth Profiling.{Zhang, 2015 #688}

To provide insight in the kinetic and thermodynamic processes in batteries it is essential to observe the Li-ion distribution depending on the electrochemical conditions and depending on the structure and morphology of the electrodes. Direct and non-destructive observation of the Li-distribution as a function of the electrode depth has been shown to be possible with Neutron Depth Profiling (NDP). Whitney et al.{S. Whitney, 2009 #6} and Nagoure et al.{S.C. Nagpure, 2014 #2;S. C. Nagpure, 2011 #7;S.C. Nagpure, 2012 #8} to use NDP to measure post mortem Lithium concentration profiles in the near surface area of commercial Li-ion batteries resulting in more insight in battery degradation after many charge/discharge cycles. Oudenhoven et al.{J. F. M. Oudenhoven, 2011 #9} performed the first in-situ NDP study on thin film solid state micro-batteries, demonstrating the direct observation of the evolution of the lithium concentration profile over time under different electrochemical conditions. Recently, Wang et al.{Wang, 2014 #653} and Liu et al.{Liu, 2014 #655}

reported on the development of in-situ NDP, they elegantly demonstrated the onset of lithiation in Sn electrodes and giving mechanistic insight in the process. Recently, we reported on extending the application of in-situ NDP towards conventional Li-ion battery systems, using the Al current collector as window, allowing to probe relatively thick electrodes with liquid electrolytes.{Zhang, 2015 #688}

By combining detailed three-phase 3D reconstruction of carbonate templated and pristine $LiFePO_4$ electrodes, using focused ion beam-scanning electron microscopy (FIB-SEM) tomography, with direct measurement of Li-ion gradients under variable conditions, using NDP, the present research reveals the origin of the improved rate performance of the template electrodes. The results give insight in the role of electronic and ionic transport in typical Li-ion battery electrodes and how the 3D electrode morphology can be tailored to improve Li-ion battery performance.

2 Experimental

2.1 Electrode preparation

The preparation method of both the conventional, referred to as standard, as well as the enhanced electrode can be found in previous work{Singh, 2013 #555} and in the supplementary information. For both electrodes the compacting pressure, current collector and compositions are the same, the difference is the 40% wt $NaHCO_3$ (Aldrich) which is added to the templated electrode slurry, which, after pressing, is allowed to react with demineralized water under the formation of water soluble NaOH and gaseous CO_2. The gas formation is visible as small bubbles are exiting the electrode, creating pores and channels that will later be filled with electrolyte.

2.2 Three Phase 3D imaging

In order to provide contrast between the present carbonous materials, in the carbon black and the PVDF binder, a two part commercial silicone resin was used in preparation for the FIB-SEM process. A more

thorough description of the sample preparation can be found in{Singh, 2013 #555} and for the FIB-SEM measurements in the supplementary information. The as-collected 2D image sequences were aligned, cropped and stacked into a 3D microstructure using a method previously described{J. R. Wilson, 2006 #28}. Each sample volume was cropped into the identical size (14.5 µm x 12.3 µm x6.4 µm, 1140 μm^3). Image segmentation was performed via multi-level Otsu's method to attribute different gray scale intensity values to different phases, where white (gray scale intensity: 255) is assigned to $LiFePO_4$ particles, gray (127) to resin-infiltrated porosity, and black (0) to carbon and binder{Otsu, 1979 #372}. It is noted that the resin-infiltrated porosity corresponds to regions which normally are occupied by the liquid electrolyte; hence this region will be referred to as electrolyte in the following text. After segmentation, the noise filter built in ImageJ (National Institutes of Health, MD, USA) was used on images that needed further noise reduction and Amira 5.5.0 (FEI Visualization Sciences Group, MA) was used for 3D visualization{Abramoff, 2004 #600}. The goal is to quantitatively analyze microstructural parameters such as volume fraction, surface area, feature size distribution, directional connectivity, tortuosity, and tortuosity distribution from 3D reconstruction volume. The 3D surface mesh was created via a marching cube algorithm to obtain the surface area{Lorensen, 1987 #652}. Interfacial surface area density (SA_I) was then calculated by normalizing the surface area of each phase to the total reconstruction volume. The feature size distribution of each phase was calculated via the method introduced by Münch et al{Münch, 2008 #88}. Connectivity and tortuosity are two important parameters that represent transport properties of the electrode, which were used to analyze electrolyte (ionic transport) and CB phase (electrical transport). The phase connectivity is determined by running a connected component labeling algorithm (function "bwlabeln" in MATLAB) through the 3D volume. By definition, there are there types of regions presented in the results. The region fully connected to target plane is defined as "Percolated", and region which touch other faces (neither source plane nor the target plane) but not the percolating volume are labeled as "Unknown". Regions that are completely

isolated from the percolating and unknown regions are defined as “Isolated”. Tortuosity and tortuosity distribution were calculated via a geometric method, namely the directional propagation method, introduced by Chen-Wiegart et al{Chen-Wiegart, 2014 #101}.

2.3 Neutron depth profiling

Neutron depth profiling was performed on one of the thermal neutron beam lines at the Reactor Institute Delft. The electrode is positioned inside the vacuum chamber at an angle of 30 degrees towards the incident neutron beam and parallel to the detector, the sample holder aperture has an area of 0.79 cm^2. ^6Li, an 7.5 % abundant isotope, is able to undergo a capture reaction in which helium and tritium ions are produced according to;

$$^6Li + n_{th} \rightarrow {}^4He(2055\,keV) + {}^3H(2727\,keV)$$

The energy that is generated by the reaction is distributed between the two particles according to conservation of energy and momentum. The ^4He and ^3H particle travel through the surrounding material during which they lose energy. By measuring this energy loss of the ^4He and ^3H particle by a charged particle implanted Si detector the depth at which the ^6Li atom was located can be determined. Separation of the ^4He and ^3H contributions, stopping power corrections and depth calibration, relating the measured 3H energy to the Li-ion depth position was performed using SRIM{Ziegler, 2010 #676} as described in detail in the Supplementary Information.

The batteries were disassembled within minutes after reaching the desired state of charge or when the voltage reached the charge or discharge cut-off voltage, 4.2 V and 2.5 V respectively. The electrode is carefully removed and rinsed using excessive amounts of dimethyl carbonate (DMC), ensuring the removal of all $LiPF_6$ salt and thereby prohibiting further charge transport between the LFP particles. Therefore, the Li-ion depth profiles in this work are only due to the Li-ions in the active material, and

hence the measured Li-concentration can be expressed in the average local Li-composition in the active material reflecting the transverse averaged state of (dis)charge of the $LiFePO_4$ as a function of depth.

3 Results and Discussions

Figure 1 shows charge voltage profiles at different charge rates and the charge and discharge capacity retention under variable rate for the standard $LiFePO_4$ and templated $LiFePO_4$ electrodes, both having tap densities close to 2.0 g/cm^3. As reported previously[21,30], templating results in lower overpotentials indicating a lower internal resistance to charge transport and consistently larger charge and discharge capacities in particular exposed at high rates.

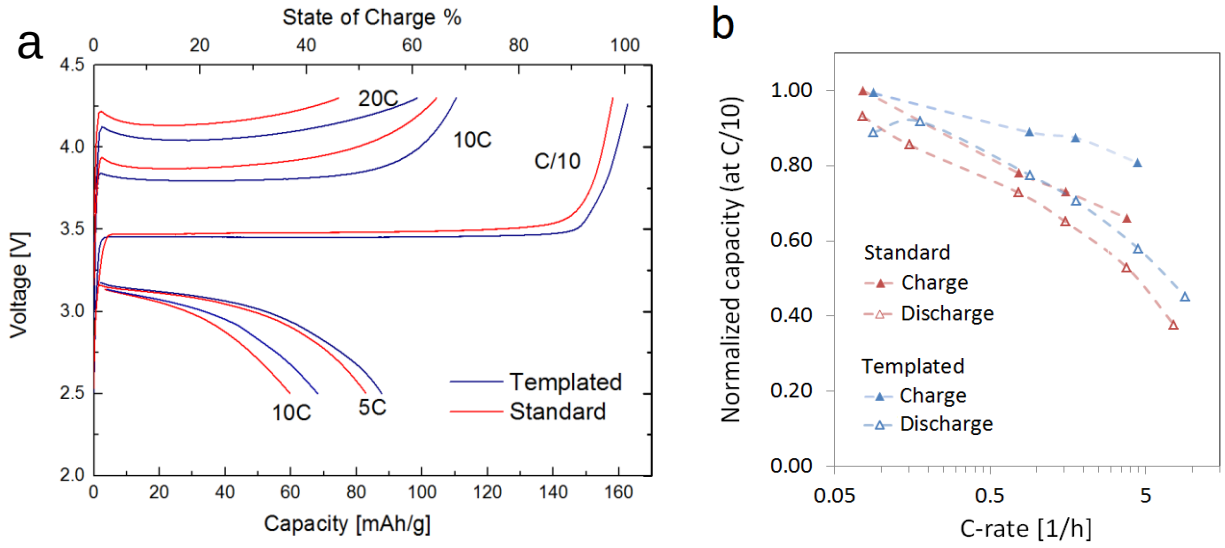

Figure 1. (a) Voltage profiles for templated and standard electrodes at different charge rates. (b) Capacity as a function of (dis)charge rate for both templated and standard electrodes.

To investigate what differences are responsible for the improved charge transport cross-sectional SEM images were obtained and the corresponding 3D reconstruction of the resin-infiltrated samples is determined, both for the templated and standard electrodes as shown in Figure 2. The silicone resin infiltration allows good image contrast among $LiFePO_4$ particles (white), carbon and binder domain (CB,

black), and resin-infiltrated pores (gray). The microstructures differ clearly in two aspects; in the templated electrodes the $LiFePO_4$ particles and carbon/binder phase are densely packed and surrounded by large micron-size pores (indicated with red dashed circle in Figure 2 (a) and (c)) accompanied by small nanometer-size pores, whereas in the standard sample all three phases were homogeneously distributed. This observation is confirmed by the cumulative feature size distributions of all three phases in both electrodes shown in Figure 3. The broad distribution in electrolyte feature size demonstrates that these pores are present throughout the analyzed volume. As expected the size distributions of the other two phases are practically identical, since the same $LiFePO_4$ and carbon powders were used in both samples. The micron-size pores are formed due to the dissolution of the $NaHCO_3$ and could play a critical role in improving rate performance in templated sample[29]. Bae et al. reported that, by introducing multiple length scales pore network, for example dual-scale porosity, the electrode kinetics can be effectively improved and result in enhanced rate performance{Bae, 2013 #471}. Random walk migration could be limited by a reduced pore size.{Saito, 2015 #680} However Fukutsuka et al. have shown that Li ion conductivities do not depend on pore size in regular free-standing membranes.{Fukutsuka, 2016 #681}

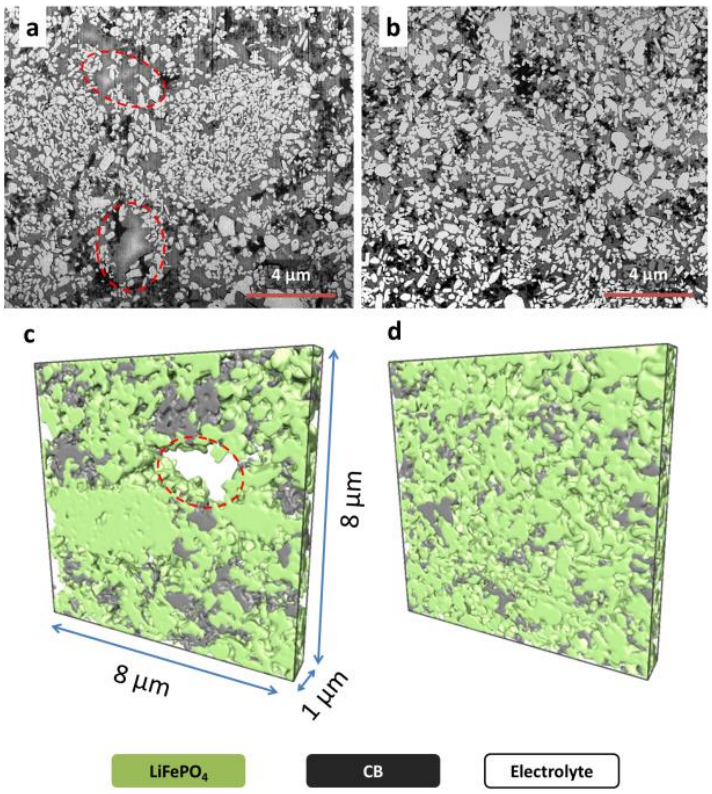

Figure 2. Cross-sectional SEM images and 3D reconstructions (a fraction of the whole reconstruction) of (a),(c) templated and (b), (d) standard cathode. The red dashed circles indicate the resin filled micron-size pores formed after dissolution of $NaHCO_3$ template.

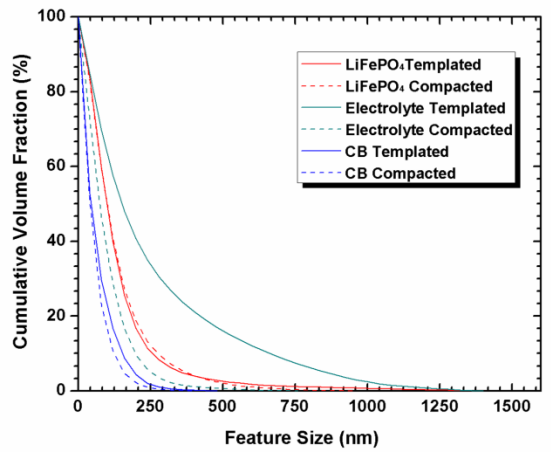

Figure 3. Cumulative feature size distribution of $LiFePO_4$, electrolyte and CB in both templated and standard electrodes.

Table 2 summarizes microstructural parameters of both electrodes obtained from the analyzed volume. The determination of the interfacial surface area is useful for accurately modeling of the charge transfer process and the strain/stress distribution in the active material during charge/discharge process{Malavé, 2014 #555;Hutzenlaub, 2014 #585;Goldin, 2012 #98;A. H. Wiedemann, 2013 #100}. Ideally one would like to maximize the interface between the $LiFePO_4$ and the electrolyte to improve ionic charge transport, as well as maximize contact of the $LiFePO_4$ with the CB to improve the electronic charge transport.

It is noted that the volume fraction calculations on each phase agree well with the values reported previously[29], which not only validates the segmentation process but also indicates that the as-obtained reconstruction volume can be obtained with excellent statistics to represent the whole electrode. For both templated and standard electrodes, the active material occupies more than 50% of the volume. Thus the templating does not negatively influence the volumetric energy density consistent with previous work[21,30]. Also a similar active fraction has previously been reported for high power commercial $LiFePO_4$ cells{Ender, 2012 #589}. Furthermore, the volume fraction of electrolyte is consistent with previous experimental results the templating method leads to a marginal (~2%) increase in porosity. The calculation of the CB volume shows nearly identical values in both electrodes. All the interphase areas are lower in the templated electrode supporting the above mentioned notion that the templated electrode is locally densely packed, whereas the standard sample is more homogenous. However, the differences are small, i.e. lower than 10%.

Table 1. Microstructural parameters calculated from $LiFePO_4$ templated and standard cathode 3D reconstruction

	Templated	**Standard**
Volume Fraction (%)		
$LiFePO_4$	50.3	52.5
Electrolyte	40.5	38.2
Carbon and Binder	9.2	9.3
Interfacial area (μm^{-1})		
$LiFePO_4$	8.25	8.93
Electrolyte	2.9	2.95
CB SA_I	5.91	6.14
$LiFePO_4$/Electrolyte	5.63	6.06
$LiFePO_4$/CB	2.62	2.87
Electrolyte/CB	0.28	0.08

In-depth knowledge of the electrode transport properties was gained via the quantitative analysis on the connectivity and tortuosity of electrolyte and CB phases. The analysis on the 3D electrolyte distance map and tortuosity distribution is shown in Figure 4. The connectivity of the percolated electrolyte volume towards the current collector is ~100% for both templated and standard electrodes, which indicates that the electrolyte accessibility in both electrodes is similar. Almost all active material particles are somewhere connected to the electrolyte. It is not known which surfaces are touching the electrolyte and this could be relevant as in LiFePO4 lithium diffusion is strictly one dimensional.{Ouyang, 2004 #683} Earlier work{Singh, 2013 #555}, using a simple model with diffusivities corrected with a Bruggeman exponent had suggested a lower tortuosity for the templated sample. However, despite the

substantial differences in electrode structure, there were no differences in the measured directional tortuosities of the electrolyte networks in the templated and standard electrodes. Although the micron-size pores (indicated in red dashed circle) are visible in the distance map of the templated sample, it does not improve the Li^+ ion diffusion significantly in terms of propagation distance. Figure 4c–d depicts the tortuosity distribution at the plane (X=14.5 μm) close to the current collector. The distributions are quite similar between two samples with the tortuosity value ranging from 1.1 to 1.3. Note that the present geometric tortuosity calculation does not account for effects of the pore size on transport properties{Kehrwald, 2011 #54} in the same way as a diffusion-based calculation or a full 3D simulation would.

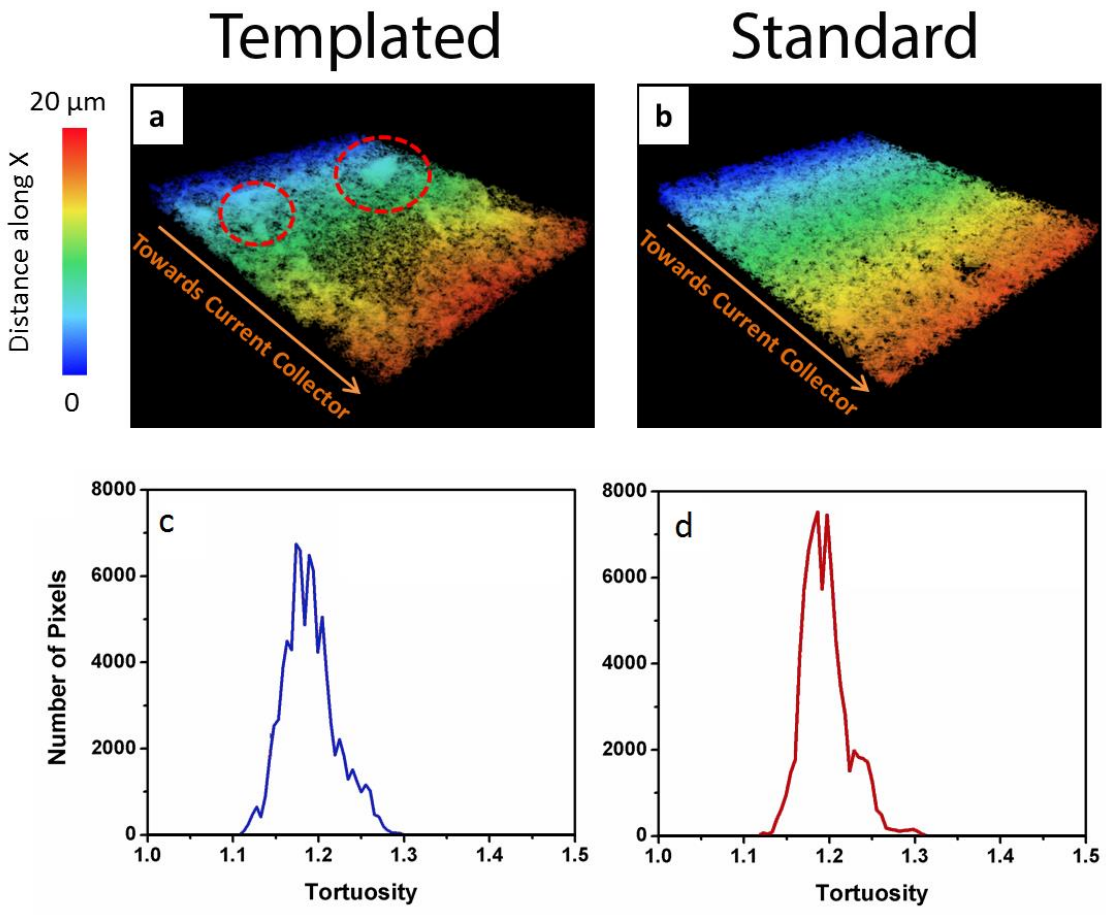

Figure 4. Three-dimensional distance map of electrolyte in the direction towards the current collector (along X direction) for (a) templated and (b) standard electrode (a thin slice along X-Z plane); (c) and (d) Histograms of the tortuosity distribution of electrolyte corresponding to X=14,5 micron, the end of the analyzed volume; Red dashed circle in (a) indicates the micron-size pores in the templated electrode.

The CB phase connectivity was significantly higher for the templated electrode (Table 1). Figure 5a-b depict the 3D reconstruction of the CB phase in the templated and standard electrode and demonstrates percolated, unknown and isolated portions. Clearly, the CB phase in the standard sample has more isolated regions (11%) than in templated sample (6.7%). These isolated regions are unfavorable, because they cannot contribute during cycling and hence result in a lower power density. This is consistent with the higher capacities achieved even at slow charging for the templated electrodes as observed in Figure 1a and consistent with NDP measurements for which also similar quantities of unreacted material have been found in empty, charged, electrodes, see figure S4.

Table 2**.** Electronic connectivity of CB phase in templated and standard electrodes

	Templated	Standard
Percolated (%)	89.2	83.6
Unknown (%)	4.1	5.4
Isolated (%)	6.7	11

The CB phase tortuosity, measured directionally towards the separator, was found to be ~36% percent lower (2.2) for the templated sample, compared to the standard sample (3.0). Figure 5c-f show the 3D distance map and spatially resolved tortuosity distribution of CB phase in templated and standard samples. The longest electron transport path in the standard sample is 55 µm, while it is 38 µm in the

templated sample. Longer electron transport distances correspond to higher tortuosity in the standard sample that will result in a higher resistance and hence larger overpotential during (dis)charge. Moreover, the CB phase tortuosity distribution in the standard sample is more heterogeneous than the templated sample. The large isolated fraction and spread in electron path length in the standard sample could explain why large local differences in the state of charge have been reported{Ouvrard, 2013 #672;Robert, 2013 #671}.

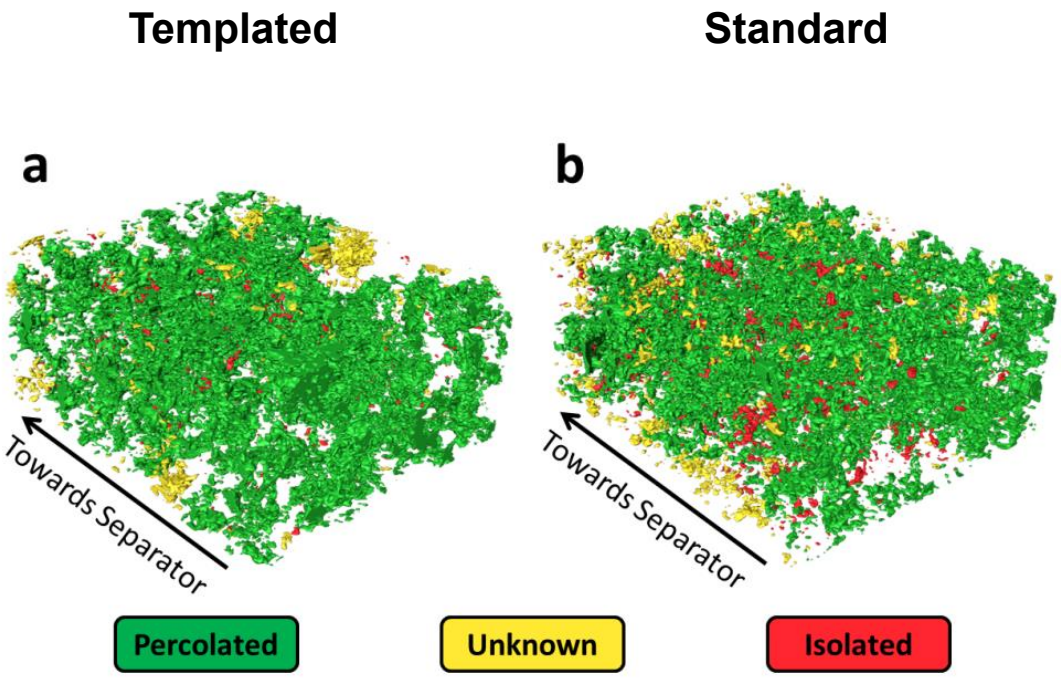

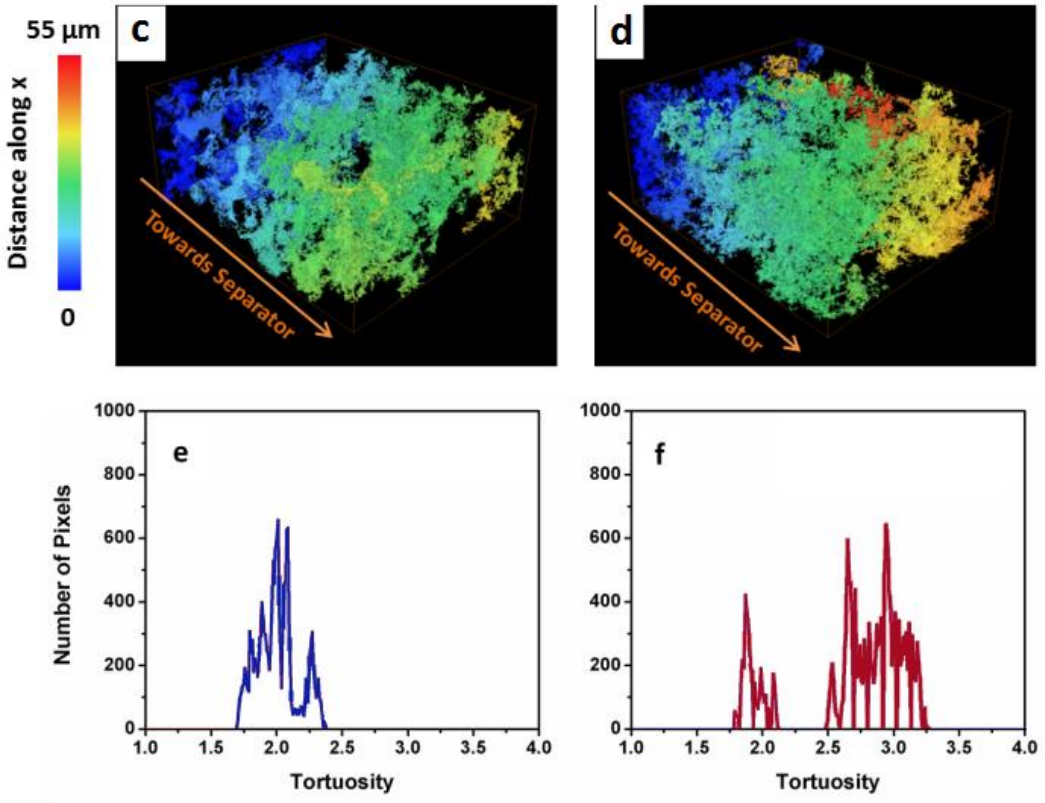

Figure 5**.** 3D image reconstructions showing the directional connectivity of the CB phase of the templated (a) and standard (b) electrode. Three-dimensional distance map of CB in the direction towards the separator (along X direction) for (a) templated and (b) standard electrons; (e) and (f) Histograms of the tortuosity distribution of CB corresponding to x=0, the start of the analyzed volume.

As the differences in terms of interfacial area and volume fractions are small, these electrodes are ideal for studying the observed differences in connectivity and tortuosity. To gain more insight in how these 3D electrode structural features influence the electrode performance, neutron depth profiling (NDP) is used; this technique allows direct, non-destructive and continuous measurement of the lithium concentration depth profile in Li-ion electrodes on the micron scale.{Oudenhoven, 2012 #477;Wang, 2014 #653;Liu, 2014 #655;Zhang, 2015 #688}. This distribution of Li-ions as a function of electrode depth reflects the in-electrode-plane averaged state of (dis)charge and allows study of electrode transport phenomena.

Previous work has shown that at high (dis)charge rates, the activity of the electrode material is limited to the part of the electrode located near the electrolyte, indicating that ionic conduction through the electrode morphology is the rate limiting charge transport mechanism[22,{Zhang, 2015 #688},24,34,{Kitada, 2016 #678;Ogihara, 2015 #679}]. This is supported by the present NDP results in Figures 6a-d showing the average state of (dis)charge as a function of electrode depth after (dis)charging with various rates until reaching the cut off voltage, for electrodes with a thickness of approximately 35 μm. After charging at 20C (Figure 6a) and after discharge at 10C (Figure 6b) and 5C (Figure 6d), the part of the electrode near the electrolyte reaches the highest state of (dis)charge. Near the electrolyte, the active material can still be supplied with Li-ions from the electrolyte (in the separator) during discharge and vice versa during charge. Further from the electrolyte, however, Li-ion transport within the electrode's electrolyte phase limits (dis)charge, leading to high internal resistance at these high rates.

In contrast to 10C discharging, at 10C charging (Figure 6c) a depth independent state of charge is observed for both the standard and templated electrodes. This indicates that the Li-ion transport through the electrolyte (located in the pores of the electrode) is better during charge as compared to discharge. Upon discharge the electrolyte at the current collector will be depleted whereas upon charge the electrolyte will be saturated. Simulations have shown that even at a relatively low discharge rate (C/7) the molarity locally could drop to 0.2 molar (starting at a 1.0 molar equilibrium concentration){Strobridge, 2015 #674}. Assuming that the electrolyte has the optimal molarity with respect to Li-ion conductivity, both depletion and saturation lead to a decrease in the ionic conductivity of the electrolyte,{Valøen, 2005 #666} depletion through the reduction in available Li-ions and saturation through the increase of the viscosity lowering the Li-ion diffusivity. As such a battery containing an electrolyte of non-optimal concentration would show either a higher charge or discharge capacity compared to a battery containing standard electrolyte, this has been recently demonstrated by Kitada et al.{Kitada, 2016 #678} It should be expected that upon electrolyte depletion (discharge) the Li-

ion conductivity will drop more dramatically, explaining the better Li-ion transport during charge which results in the higher state of charge reached at fast charging as compared to discharging (see Figure 1).{Roberts, 2014 #667}

Consistent with the electrochemical results in Figure 1 {Singh, 2013 #613;Singh, 2013 #555} the depth dependent state of (dis)charge shown in Figures 6a-d display a larger state of (dis)charge after high rate (dis)charge throughout the electrodes. Figures 6a and 6b proves that templating improves the state of (dis)charge both near the current collector and near the electrolyte, indicating that not only the Li-ion transport is improved, but also the electronic transport. Although the templating does not improve the tortuosity of the porous electrolyte network, as concluded from the 3D image reconstruction result in Table 2, it is possible that the presence of larger voids, introducing multiple length scales pore network, may be responsible for the better ionic transport{Bae, 2013 #471}. As discussed above, during discharge the improved ionic transport is not effective, most likely because of depletion of the electrolyte. The increase in state of (dis)charge near the electrolyte side indicates that templating also improves electronic transport. For 20C charge the state of charge throughout the electrode is enhanced by the templating whereas on 10C and 5C discharge templating mainly improves the state of discharge near the electrolyte side requiring an improved electronic connection with the current collector. Indeed templating results in a significantly better tortuosity of the CB network as observed in Figure 6, which appears in large part to be the origin for the higher charge capacity of the templated electrodes.

In Figure 6e-f the state of (dis)charge profiles are shown at approximately 50% state of charge and discharge at C/5 for both electrodes. The absence of a distribution in the state of (dis)charge as a function of depth in the templated electrodes confirms the better charge transport characteristics due to the templating. An interesting observation is that at C/5 charging the gradient in the standard electrode is reversed compared to 10C charging shown in Figure 6a. Apparently, it is easier to delithiate

the current collector side of the electrode, indicating that electronic transport is limiting at C/5 where Li-ion transport appears limiting at 20C. This is consistent with recent findings where it was shown that the rate limiting process actually depends on the (dis)charge rate, for the considered $LiFePO_4$ electrodes being nucleation at low rates, ionic transport through the electrolyte in the pores of the electrode at high rates, and electronic transport limitations at medium rates{Zhang, 2015 #688}. Recently Li et al.{Li, 2015 #745} also indicated that electronic transport may be rate limiting at specific conditions, demonstrating that the most resistive process in a $LiFePO_4$ electrode appears to be the electronic conduction between the $LiFePO_4$ particle surface and the nearest branch of the percolating carbon network. An interesting observation in Figure 6f is the maximum in the state of discharge of the standard electrodes during C/5 discharge. This reflects the competition between ionic and electronic transport, apparently having a similar resistance at this discharge rate and for this specific electrode (3D structure and thickness). Again reflecting the differences between charge and discharge, demonstrating the importance of ionic limitations even at low discharge rates.

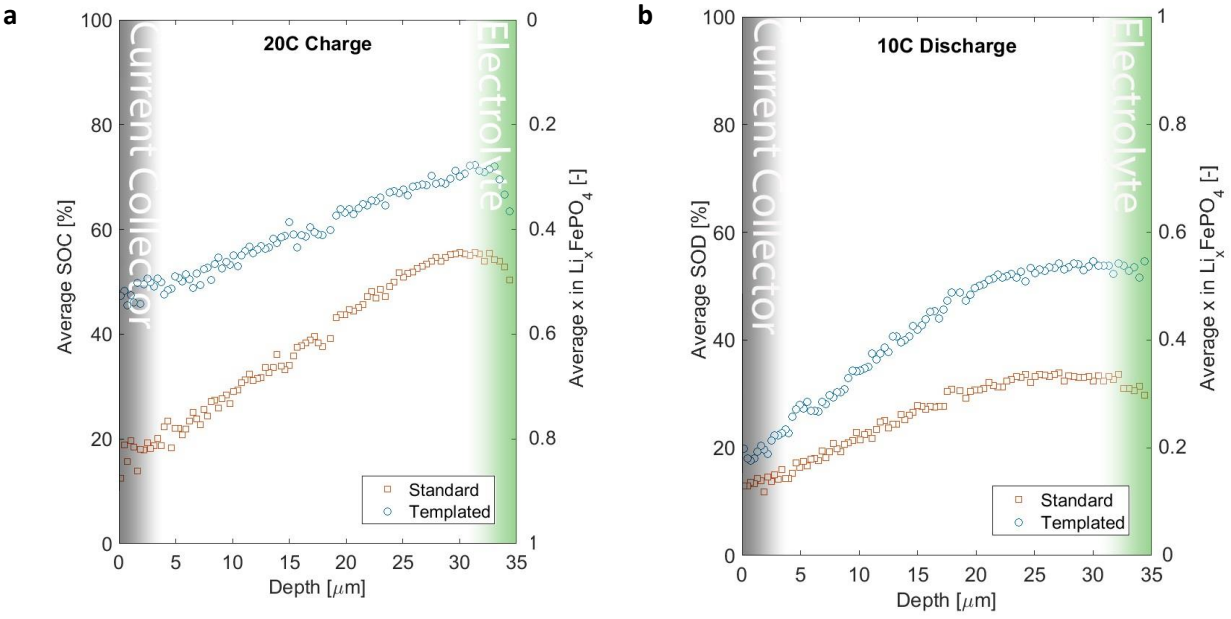

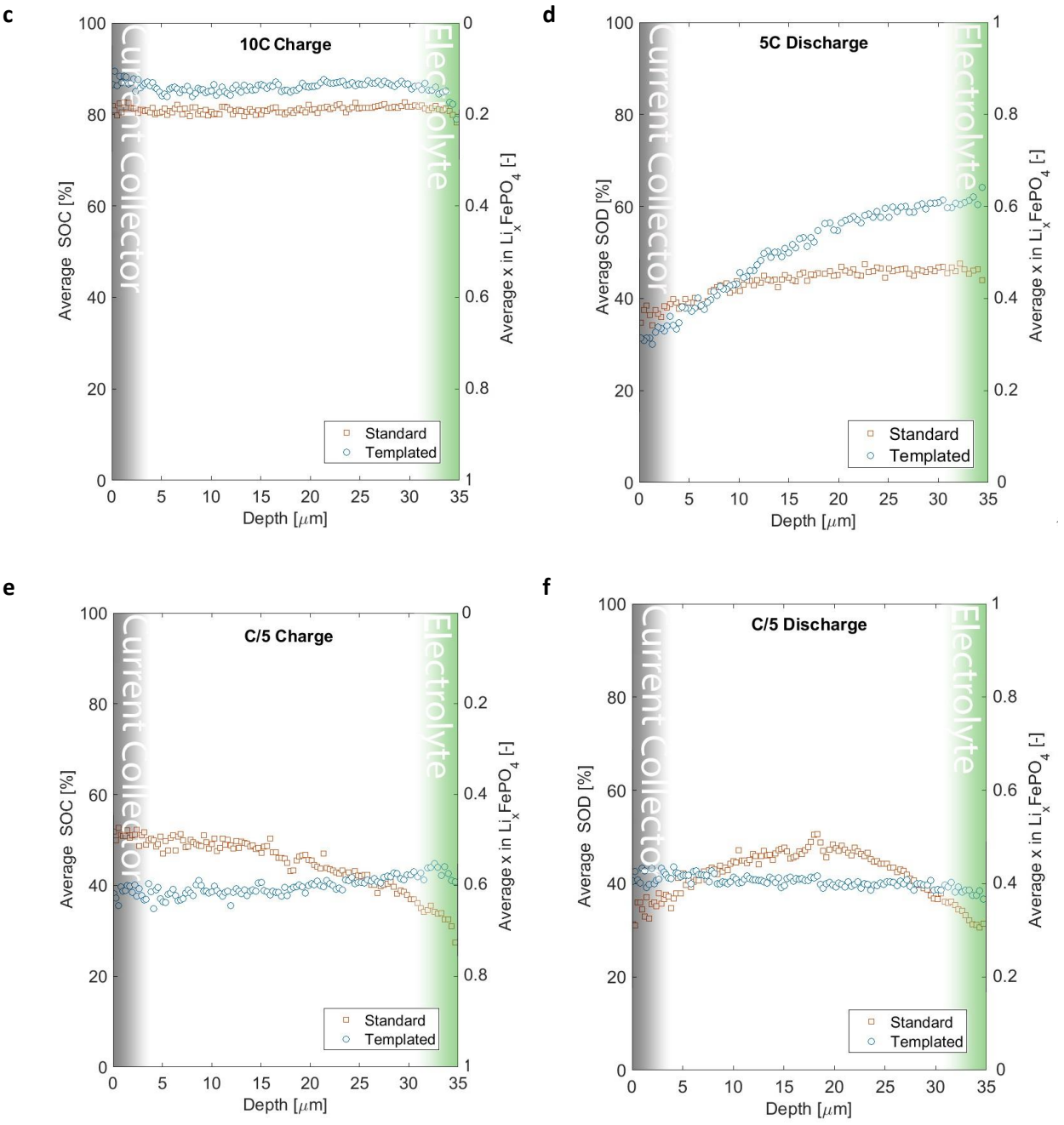

Figure 6. (a-d) State of (dis)charge profiles after cycling at high rates for both templated and standard electrodes. (6e-f) State of (dis)charge profiles at approximately 50% state of (dis)charge during C/5 (dis)charging. The grey shade marks the location of the current collector and the green shade at approximately 35 μm the interface with the electrolyte.

4 Conclusions

Three-phase 3D reconstruction using FIB-SEM has been employed to investigate the origin of the improved rate performance of $LiFePO_4$ templated electrodes as compared to standard $LiFePO_4$ electrodes. Microstructural parameters were determined, including volume fraction, surface area, and feature size distributions of the active $LiFePO_4$ material, CB and the porous structure, where the latter is filled with electrolyte during battery operation. Due to the analogous electrode formulations most of these parameters, including the interphase areas, are found to be similar this represents an almost ideal case study for direct comparison between the tortuosity and connectivity of templated and non-templated electrodes giving unique insight in the origin of the differences in electrochemical performance, and more general in the relation between the electrode morphology and battery performance.

The CB and electrolyte connectivity, tortuosity, and tortuosity distributions were analyzed for both electrodes from the 3D images and compared. The connectivity calculation shows a fully percolated electrolyte phase for both templated and the standard electrodes. For the tortuosity in the electrolyte phase no significant differences were found between the two electrodes in contrast to what was concluded previously{Singh, 2013 #613;Singh, 2013 #555}. Nevertheless it is proposed that the hierarchical interconnected porosity in the templated electrodes improves the ionic transport throughout the electrodes, partially responsible for the better rate performance. This is especially observed upon charge where direct observation of the average state of charge as a function of depth in the electrode by NDP reveals that, compared to the standard $LiFePO_4$ electrodes, the templated electrodes show much more charge activity near the current collector side. This is much less obvious during discharge, most likely due to electrolyte depletion reducing the conductivity of the electrolyte, the apparent origin of the asymmetric charge-discharge performance.

Although the same amount of CB was used in both electrode formulations , the connectivity calculation based on the three-phase 3D reconstruction reveals that the CB network is more percolating in the templated electrodes, which must result in a higher electrical conductivity. Moreover, the tortuosity distribution of the electronic network is more homogeneous in the templated electrode making a larger part of the active material well connected to the CB network. This demonstrates that a lower electronic resistivity of the templated electrode is for a large part responsible for the improved capacities during charge and discharge at high rates. This is consistent with the larger charge and discharge activity in the templated electrode near the electrolyte/separator directly observed with NDP. The shift of the most active electrode region from the current collector side towards the electrolyte/separator side upon higher (dis)charge rates is consistent with recent findings{Zhang, 2015 #688}, indicating that the rate limiting step for the charge transport in electrodes depends on the (dis)charge rate itself.

These results illustrate that typical electrodes have a far from optimal charge transport network, and that surprisingly the carbonate templating method results in a better electronic conductive CB network, in a large part responsible for the improved rate performance. Further improvement of the ionic and electronic network appears possible, signifying the importance of developing cheap and upscalable methods to improve the charge transport in electrodes that will enable improved power and energy density of Li-ion batteries.

Acknowledgement

The research leading to these results has received funding from the European Research Council under the European Union's Seventh Framework Program (FP/2007-2013) / ERC Grant Agreement no. [307161] of MW.

References